Interaction between Asphaltenes and Fatty-alkylamine Inhibitor in Bulk Solution

Sreedhar Subramanian*, Sébastien Simon and Johan Sjöblom

Ugelstad Laboratory, Department of Chemical Engineering, Norwegian University of Science and Technology (NTNU), N-7491 Trondheim, Norway.

*Corresponding author: E-mail: sreedhar.subramanian@ntnu.no , Tel: (+47) 73 59 41 59

ABSTRACT

In the present work, the mechanism of interaction (and precipitation inhibition) between asphaltenes and a commercial fatty alkylamine inhibitor is investigated by a combination of techniques: "macro" properties such as the asphaltene flocculation/precipitation onset and the amount of asphaltene precipitated are measured in combination with the heat of interaction between asphaltenes and inhibitor determined by isothermal titration calorimetry (ITC). Asphaltene fractions as well as esterified asphaltenes were also used to pinpoint the mechanism.

ITC shows that only a small fraction (around 6%) of asphaltenes interacts strongly with the inhibitor, while the remaining asphaltenes exhibit much weaker interactions. This proportion is higher in the fraction called *irreversibly-adsorbed* asphaltenes, which was prepared by adsorption of asphaltenes onto calcium carbonate. These 6% are mostly composed of acidic asphaltenes (as indicated by the measured acid-base interaction).

However, the acid-base interaction was not found to be the main interaction responsible for the inhibition of asphaltene precipitation induced by the inhibitor, based on determination of precipitation onset and amount of asphaltene precipitated. Other type(s) of interaction is/are responsible for the inhibition properties of the inhibitor. These interactions are not detected by ITC. The nature of other interactions is not known for the moment, but it was shown that *irreversibly-adsorbed* asphaltene fraction contains a higher concentration of the functionality (ies) responsible for the "other" type of interaction.

1 Introduction

Asphaltenes represent the heaviest and the most polar component of crude oil. They are defined primarily as a solubility class: insoluble in n-alkanes (eg. n-heptane or n-pentane), but soluble in aromatic solvents like toluene or xylene.[1] Asphaltenes have an average molecular weight of 750 g/mol, with a majority of molecules within the range of 500-1000 g/mol and are composed of polycyclic aromatic hydrocarbons (PAH) with alkyl chains along their periphery.[2] In addition, asphaltenes also contain small amounts of heteroatoms including oxygen, nitrogen, sulfur and trace metals. The tendency of asphaltene molecules to aggregate is attributed to the π-π interactions (the intermolecular between the aromatic cores of asphaltenes), hydrogen bonding between the functional groups and acid-base interactions.[3-4]

Asphaltenes exist in the form of a colloidal dispersed state in the crude oil, and are believed to be stabilized and/or solubilized by resins.[5-6] The changes in pressure and/or oil composition during production and transport of crude oil can destabilize the dispersion medium, thereby leading to precipitation of asphaltenes.[6] In order to prevent asphaltene precipitation, amphiphilic molecules can be added to the crude oil.[7] The amphiphile typically consists of a polar functional group that interacts with the asphaltenes, and a non-polar alkyl chain which facilitates in solubilization of the asphaltenes.[8] Studies by Chang et al.[9] showed that the effectiveness of the amphiphile depends both on the polarity of the head group and the length of alkyl chain. Increasing the acidity or basicity of the amphiphile head group facilitates acid-base interaction between the asphaltene and inhibitor. Hence alkylbenzene derived amphiphile like dodecylbenzene sulfonic acid (DBSA) has been found to be effective in stabilizing asphaltenes.[9-10] Alkyl phenols like nonyl phenol (NP) also act as effective asphaltene stabilizers. Alkylphenols interact with asphaltenes via hydrogen bonding between amphiphile and the interaction sites (-OH and –N) of asphaltenes located at periphery.[11] The superior solubilizing ability of DBSA has been attributed to the presence of a larger and more polar sulfonic acid (-SO_3H) group in DBSA than compared to the hydroxyl (-OH) group in alkylphenol.[12] However, DBSA was found to be ineffective for peptizing Cold Lake asphaltenes while NP was effective. This behavior is not understood.[13]

The asphaltene-amphiphile interaction has been explained to proceed via a two-step process. The amphiphile initially interacts with asphaltenes and adsorbs onto the surface of asphaltene. This is followed by the interaction between the adsorbed amphiphiles, thereby resulting in the formation of hemimicelles on the surface of asphaltenes.[14] Adsorption studies

indicate that DBSA adsorbs perpendicularly to asphaltene surface due to stronger interaction of polar head, while NP tends to have a parallel orientation to asphaltene surface due to dispersive type interactions.[14] Amphiphiles with linear alkyl chain containing more 16 carbons have a tendency to crystallize. Hence, branched double tails are used as an alternative to overcome the problem.[15] The effectiveness of inhibitor is also dependent on their concentration. Based on fourier transform infrared (FTIR) measurements, it was found that DBSA interacts with the basic groups and C=C bonds present in asphaltenes and adsorbs irreversibly on the asphaltene surface.[9] At low inhibitor concentrations, the DBSA-asphaltenes interaction leads to formation of salt of lower solubility, thereby causing a precipitation earlier than observed with asphaltenes.[6] Thus DBSA is effective only at higher concentrations.[6, 16-17] However, certain inhibitors at high concentrations tend to have a dominance of inhibitor-inhibitor interaction (self-aggregation) in the bulk solution over asphaltene-inhibitor interaction, thereby reducing inhibitor effectiveness.[18]

Isothermal titration calorimetry (ITC) has been previously used as a tool to characterize the interactions between asphaltenes and inhibitors (DBSA, NP).[19-20] Attempts to model the interaction between asphaltenes and inhibitors was less successful due to assumptions made in interaction enthalpy and association constant in order to fit the experimental data. However ITC measurements have been successful in predicting the number of active sites per asphaltene molecule which are capable of interacting with NP, thereby forming (Asp)(NP) and $(Asp)(NP)_2$ complexes.[19] The interactions between asphaltenes and DBSA are however more complex, and dependent on both the self-aggregation of DBSA and concentration of asphaltenes in solution.[20]

In the present work, the bulk interactions between asphaltenes and a commercial fatty alkylamine inhibitor is investigated. Near infrared (NIR) spectroscopy was used to determine the ability of the inhibitor to delay the precipitation onset of asphaltenes in model oil (toluene/n-hexane mixtures), while ITC was utilized for probing the interaction between inhibitor and asphaltene. Calorimetric studies were further extended to study the interaction of inhibitor with the most polar asphaltene sub-fractions (*irreversibly-adsorbed* asphaltenes and asphaltene *3.5V*) obtained from fractionation techniques described in our earlier publications.[21-22] The i*rreversibly-adsorbed* asphaltenes represent the fraction of asphaltenes which interacts strongly with calcium carbonate, and can be recovered only by dissolution of $CaCO_3$ using an acid, while asphaltene *3.5V* is the asphaltenes precipitated when crude oil

was diluted with 3.5 volume of n-hexane/g of crude oil. Finally, an attempt has been made to identify the functional group in asphaltene which interacts strongly with the inhibitor by esterifying asphaltenes.

2 Experimental Section

2.1 Chemicals

2.1.1 Asphaltene preparation

Several asphaltene fractions and asphaltene derivatives were considered in the present work. Asphaltenes were extracted from a chemical free crude oil from Norwegian Continental Shelf based on a 40 times dilution ratio (volume of n-hexane/mass of crude oil). The characteristics of the crude oil and asphaltenes along with the procedure used to extract asphaltenes can be found in our earlier publications.[21-22] Asphaltenes obtained from this procedure are called "*whole* asphaltenes".

Whole asphaltenes were fractionated into 3 fractions by adsorption onto calcium carbonate according to a procedure developed and described by Subramanian et al.[21] Only the most strongly adsorbed fraction was studied in the article. This fraction, named as *irreversibly-adsorbed* asphaltenes (abbreviated *irre-ads*) represents 21 wt% of the *whole* asphaltenes as determined by gravimetry.

A third sample named asphaltenes *3.5V* was also studied in the article. It is the first fraction precipitating from crude oil when diluted with moderate amounts of n-hexane. It is obtained by adding 70 ml of n-hexane to 20 g of crude oil (or 3.5vol/g of crude oil). The fraction is obtained after filtration and drying, and represents 28 wt% of the *whole* asphaltenes. The preparation procedure and comparison of composition and bulk and adsorption properties of *irreversibly-adsorbed* asphaltenes and asphaltenes *3.5V* is given in Subramanian et al.[22]

Asphaltenes were also esterified by methanol using sulfuric acid as catalyst according to a procedure described in Simon et al.[23], Pradilla et al.[24] and Nasir et al.[25] This asphaltene derivative was named *ester*-asphaltenes. Every batch of *ester*-asphaltenes prepared was characterized by fourier transform infrared (FTIR) spectroscopy and interfacial tension (IFT) measurements. The FTIR spectrum of *ester*-asphaltenes shows the appearance of a small peak at around 1736 cm^{-1}, which is absent in the case of *whole* asphaltenes. The interfacial

tension between 1g/L *ester*-asphaltenes and pH=10 buffer solution measured with a Sinterface PAT-1M tensiometer is 24 mN/m, contrary to 12 mN/m for *whole* asphaltenes. These data are in agreement with the data obtained by Simon et al.[23], and show that the esterification was successful.

2.1.2 Other chemicals

N-hexane (VWR, >97%) and anhydrous toluene (Sigma Aldrich, 99.8%) was used for near infrared (NIR) spectroscopy measurements. The solvent used for ITC experiments was xylene (VWR, >98.5%). A commercial fatty alkylamine-based inhibitor (molecular weight ≈ 1000 g/mol) was provided by AkzoNobel Surface Chemistry AB (Sweden).

2.2 Experimental techniques

2.2.1 Near infrared (NIR)

NIR spectroscopy was used to determine the asphaltene precipitation onset in mixtures of toluene and n-hexane.

2.2.1.1 Asphaltene solutions without inhibitor

In the case of *whole* and *ester* asphaltenes, 40 g/L asphaltene stock solution in toluene was first prepared separately and sonicated for 30 minutes before aging overnight. The asphaltene solution was then diluted with pure toluene and pure n-hexane to obtain 2 g/L asphaltene solutions at different toluene/n-hexane ratios. For the asphaltene fractions *irre-ads* and asphaltene *3.5V*, the stock solution in toluene was 20 g/L, and it was diluted to a final concentration of 1 g/L at different toluene/n-hexane ratios.

2.2.1.2 Asphaltene solutions with inhibitor

For *whole* and *ester* asphaltenes, 40 g/L asphaltene stock solution and 40 g/L inhibitor solution in toluene was prepared separately. The solutions were sonicated for 30 min before aging overnight. The next day, the asphaltene and inhibitor solutions were mixed in equally (by weight) to obtain a mixed solution containing 20 g/L asphaltenes + 20 g/L inhibitor. The solutions were sonicated for 30 min before aging overnight. The mixed solution was then diluted with pure toluene and pure n-hexane to obtain 2 g/L asphaltene solutions at different toluene/n-hexane ratios. For the asphaltene fractions *irre-ads* and asphaltene *3.5V*, the stock asphaltene solution was 20 g/L, while the mixed asphaltene-inhibitor solution was 10 g/L asphaltenes + 10 g/L inhibitor. The mixed solution was diluted to a final concentration of 1 g/L at different toluene/n-hexane ratios.

The absorbance of all the asphaltene solutions was measured at 1600 nm at 1h and 1day after addition of n-hexane to see the influence of aging on precipitation onset. In case of whole asphaltenes, NIR measurements were also done after 3 days to study the effect of aging. The samples were also observed by microscopy (DVM Nikon Eclipse Video Microscope) after 1h and 1 day to confirm the presence of asphaltene precipitates.

2.2.2 Quantification of amount of precipitated asphaltenes

The amount of asphaltenes precipitated was determined according to the following procedure: The 2 g/L whole and ester asphaltene solutions at different toluene/n-hexane ratios were prepared (both with and without inhibitor) in the same way as mentioned in the previous NIR section (2.2.1.1 and 2.2.1.2). The 2 g/L asphaltene solutions were then stirred for 24 hours at room temperature (~22°C) and centrifuged at 4000 rpm for 30 min. The supernatant was recovered and filtered with a 0.45 µm PTFE filter (Millipore). After evaporation of the solvent (present in supernatant solution), the asphaltenes were dissolved in a known volume of pure toluene and their concentrations were determined by measuring the absorbance at both λ=336 nm and 500 nm using a calibration curve built beforehand. It has been checked that the tested inhibitor does not absorb at these wavelengths.

2.2.3 Isothermal Titration Calorimetry (ITC)

ITC was used to measure the heat of interaction between asphaltenes or asphaltene fractions and the commercial inhibitor. The measurements were done using a NANO ITC Standard volume from TA Instruments (New Castle, DE, USA) fitted with a 250 µL syringe and a 943 µL measuring cell. The calorimeter was periodically calibrated by titrating a Tris base solution with a 1 mM HCl solution, and comparing the heat of reaction with the literature values.

Asphaltene solutions were prepared by dissolving asphaltenes (or asphaltene fractions) in xylene to get a concentration of 10 g/L. Then, the mixture was sonicated for 30min and left overnight. The solution was again sonicated for 30 minutes before being loaded into the calorimeter cell. Inhibitor stock solution was prepared by dissolving desired amount of inhibitor in xylene to get inhibitor solutions of 2, 4 or 10 g/L concentration. The solution was aged overnight before being loaded into the calorimeter syringe.

The ITC experiment was set to begin when the standard deviation of the baseline was lower than 0.01 µW and the slope lower than 0.1 µW/h. Experiments were performed by injecting the inhibitor solution present in the syringe into the asphaltene solution present in the cell by step of 10 µL at a temperature of 25°C and a stirring rate of 250 rpm. The interval between injections was varied between 400s and 2700s to allow equilibration. A 300s baseline was collected before the first and after the last injection. The data was collected and analyzed with the NanoAnalyze software (TA instrument).

3 Results

As mentioned in the introduction section, the goal of this article is to determine the nature of interactions between asphaltenes and a fatty amine-based inhibitor, and their consequences on the precipitation of asphaltenes. The strategy adopted was to fractionate or chemically modify asphaltenes to accurately pinpoint which asphaltene functionality interacts the most with the fatty alkylamine-based inhibitor. The main technique used to characterize interactions was ITC, while the precipitation onset and the percentage of asphaltene precipitated were determined to characterize the consequences of asphaltene-inhibitor interactions.

3.1 Interactions between inhibitor and *whole* asphaltenes

3.1.1 Effect of inhibitor on *whole* asphaltene precipitation onset

The first part of the study aims to determine the ability of the commercial inhibitor to influence the asphaltene precipitation onset.

Figure 1 presents the determination of the precipitation onsets of asphaltenes in mixtures of toluene and n-hexane, in absence of inhibitor measured 1h, 1 day and 3 days after addition of n-hexane into the stock *whole* asphaltene solution in pure toluene. The three curves present similar aspects with a constant value of optical density at low hexane content followed by a steady increase of optical density above critical n-hexane content. This increase is due to scattering of NIR beam by large particles in solution. Consequently, the critical n-hexane content at which optical density increases is the precipitation onset. Even if it can be difficult to determine the exact vol% hexane at which the optical density starts to increase, it seems that the precipitation onset is comprised between 60 and 65 vol% after 1h and decreases to between 55 to 60 vol% after 3 days. Concomitantly, the optical density increases with time at constant n-hexane content values above the precipitation onset, which indicates

that the asphaltene floc size or the amount of precipitated asphaltenes increases with time. These results are consistent with previous microscopy data obtained by Maqbool et al.[26], who showed that the precipitation onset depends on time. Indeed, in toluene, asphaltenes form most likely a mixture of nanoaggregates and monomers. When hexane is added, these asphaltenes flocculate to create increasingly bigger objects until forming micrometer-sized flocs. This aggregation kinetics is either diffusion limited or reaction limited (DLA or RLA) as demonstrated by Yudin et al.[27-28] Consequently, it takes time before the increase of asphaltene size is detected by the used method, and the precipitation depends both of ageing and detection technique.

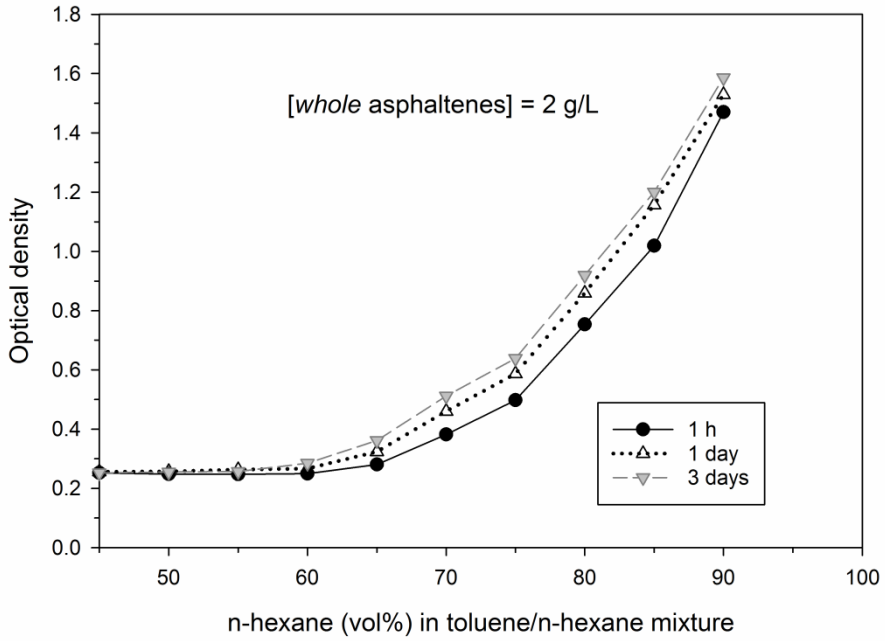

Figure 1: Flocculation onsets of *whole*-asphaltenes (2 g/L) in mixtures of toluene and n-hexane determined at 1600 nm 1h, 1 day and 3 days after addition of n-hexane.

Figure 2 shows the determination of the *whole* asphaltenes precipitation onset in presence of various concentrations of inhibitor. More hexane is required to induce the precipitation of asphaltenes in presence of inhibitor: Indeed, the flocculation/precipitation onset increases from 60-65 vol% n-hexane without inhibitor to 65-70 vol% and 70-75 vol% at 0.8 and 2 g/L inhibitor concentration respectively. Moreover, at a given hexane content (vol%) and above the precipitation, the optical density decreases in presence of inhibitor. This indicates that there are less and/or smaller asphaltene colloids dispersed in toluene. All these observations confirm the efficiency of the inhibitor to reduce the precipitation of

asphaltenes. It can be noticed that the inhibitor concentration must be the same order of magnitude as the asphaltene concentration to obtain a noticeable increase of the precipitation onset (here ca. 10 vol% hexane difference for 2 g/L of asphaltenes and inhibitor).

Figure 2 must be compared to figure 3 which presents the percentage of *whole* asphaltenes precipitated with and without inhibitor at various toluene/n-hexane ratios. The curves present the following shape: Initially, at low n-hexane content, no asphaltene is precipitated. Then, above a critical n-hexane content (i.e., the precipitation onset), some asphaltenes start to precipitate out of solution, and the percentage of precipitated asphaltene increases nearly linearly with the n-hexane content. The precipitation onsets determined by this method seems to be in good agreement with the values determined by NIR for the same contact time (figure 2). The effect of the inhibitor is clearly visible on figure 3: not only the precipitation onset increases but also the percentage of precipitated asphaltenes at a given n-hexane content is systematically lower in presence of inhibitor. The curves presented in figure 3 are reminiscent of results concerning the increase of asphaltene solubility by resins (the second most polar fraction of crude oil)[29], and several authors have suggested that inhibitors act similarly as resins.[30-32]

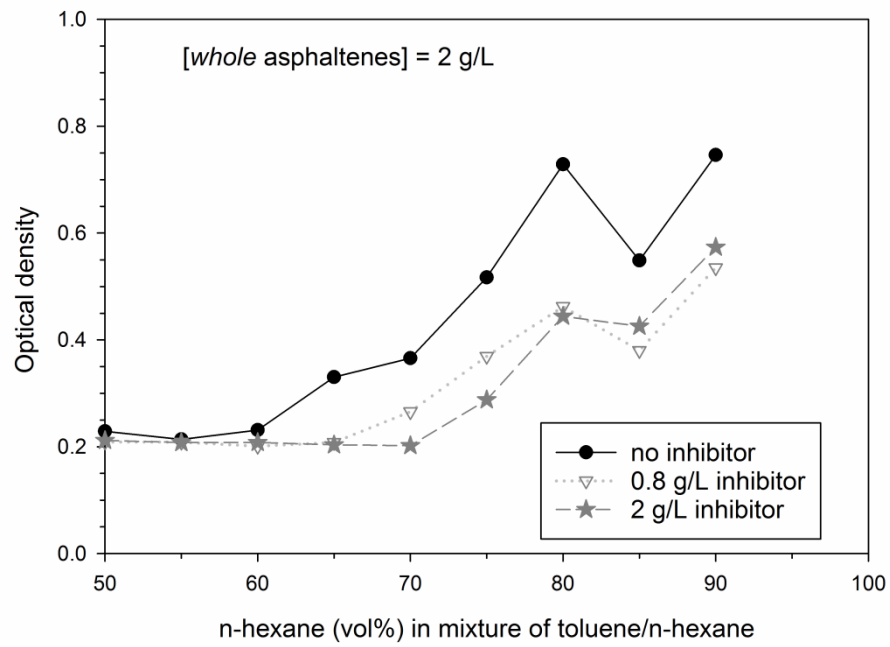

Figure 2: Determination of the precipitation onset of *whole* asphaltenes (2 g/L) in mixtures of toluene and n-hexane in presence of various concentrations of inhibitor. Measurements

performed 1 day after hexane addition at 1600 nm. The experiments were performed with a asphaltene different batch than in figure 1.

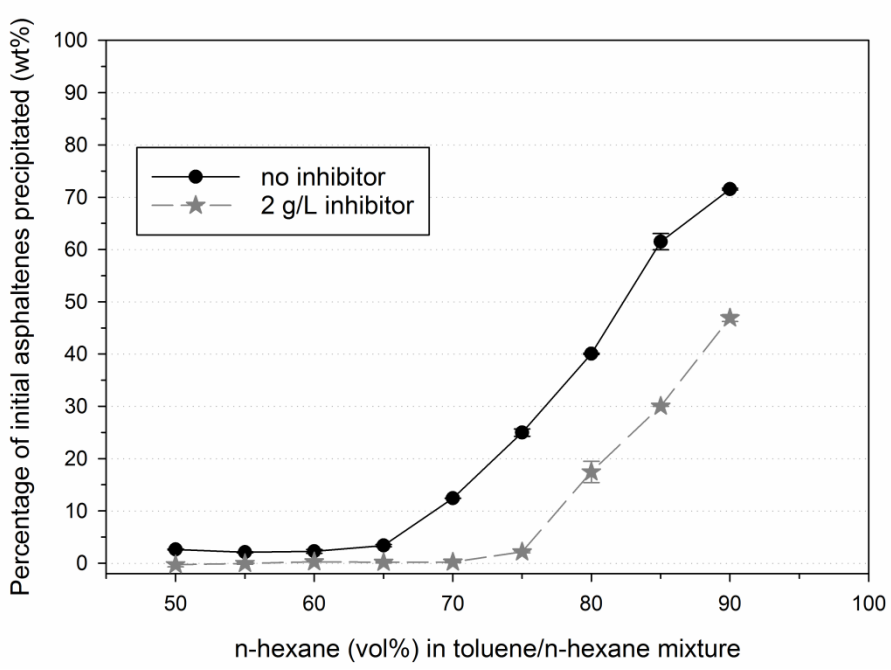

Figure 3: Percentage of *whole*-asphaltenes precipitated with and without inhibitor at various toluene/n-hexane ratios. Initial concentration of *whole* asphaltenes was 2 g/L.

3.1.2 Interactions between asphaltenes and inhibitor studied by ITC

After determining the effect of the fatty-alkylamine based inhibitor on a macroscopic property of asphaltenes (precipitation), ITC was used to probe the molecular interactions between asphaltenes and inhibitor. Figure 4 presents examples of ITC data showing the method used to determine the net interaction heat between asphaltenes and inhibitor. There are three major contributions to the heat measured when an asphaltene solution is titrated by a solution of inhibitor (ΔH_{Total}):

-The first one corresponds to the dilution of asphaltenes (ΔH_{Asp}). This dilution induces a dissociation of asphaltene aggregates. This dissociation is endothermic as previously demonstrated.[20]

-The second one accounts for the dilution of inhibitor (ΔH_{Inh}). Figure 4 shows that the dilution is an endothermic process which presumably originates from the dissociation of inhibitor aggregates. The enthalpy data of inhibitor dilution can be satisfactory fitted with a model assuming that inhibitors form dimers in solution which are partially dissociated during dilution as shown with the following equations:

$$(\mathrm{Inh})_2 \leftrightarrow 2\mathrm{Inh} \quad (1)$$

$$\mathrm{K_d} = \frac{[\mathrm{Inh}]^2}{[(\mathrm{Inh})_2]} \quad (2)$$

where $[(\mathrm{Inh})_2]$ represents inhibitor dimer concentrations, [Inh] represents inhibitor monomer concentrations, and $\mathrm{K_d}$ is the dimer dissociation constant. The fitted inhibitor dilution enthalpy curves is presented in figure 4, and the determined value of $\mathrm{K_d}$ and dissociation enthalpy $\Delta\mathrm{H_d}$ and entropy $\Delta\mathrm{S_d}$ are given in table 1. The fact that these values are independent of the concentrations (even if $\mathrm{K_d}$ presents a slight increase with concentration) is a good indication of the validity of the dimer model to the inhibitor self-association properties in xylene.

-Finally the last one corresponds to the interactions between asphaltenes and inhibitor (ΔH_{Int}). Inter alia, the heat accounting only for the interactions between asphaltenes and inhibitor can be deducted with the following equation:

$$\Delta\mathrm{H_{Int}} = \Delta\mathrm{H_{Total}} - \left(\Delta\mathrm{H_{Asp}} + \Delta\mathrm{H_{Inh}}\right) \quad (3)$$

The interactions between asphaltenes and inhibitor are significant since interaction heat is not equal to zero. Moreover, the negative heat values obtained indicate that the interactions are exothermic.

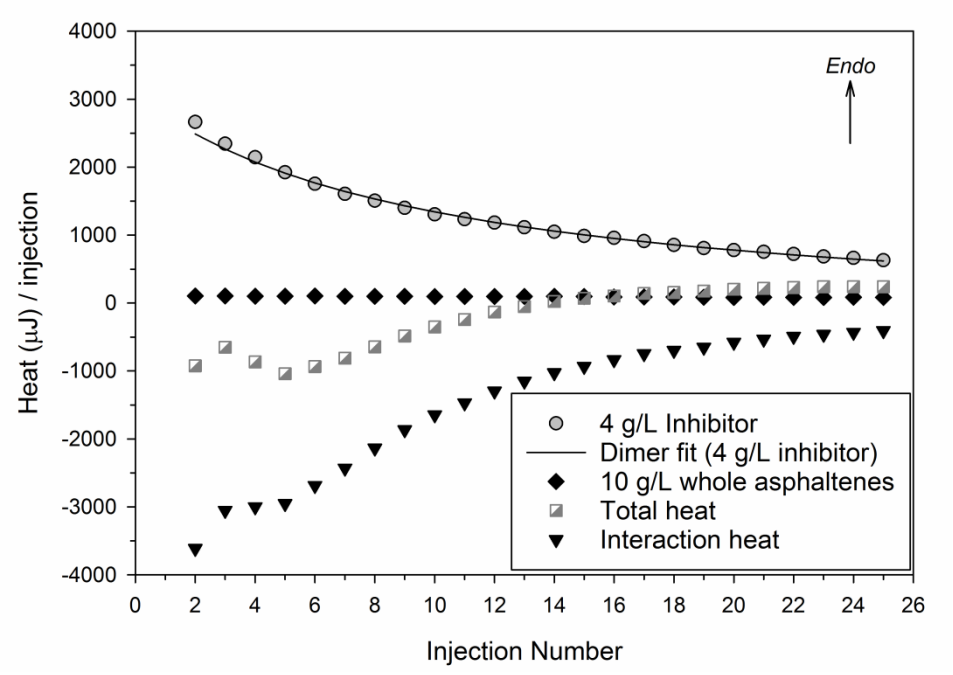

Figure 4: Example of typical results showing the heat contributions of all the major processes occurring when injecting 4 g/L inhibitor solution into 10 g/L *whole* asphaltene solution (solvent: xylene). Contributions shown: dilution of whole asphaltenes (10 g/L); dilution of

inhibitor (4 g/L); titration of whole asphaltenes (10 g/L) by inhibitor (4 g/L) and the calculated interactions between whole asphaltenes and inhibitor determined by Eq. (3). The values for the dilution of inhibitor are fitted with a dimer model. Note: The heat values corresponding to first injection are not used for data analysis to account for dilution effects, and hence not shown in the graph.

[Inhibitor] g/L	2	4	10
K_d	0.0015 ± 0.0001	0.0016 ± 0.0001	0.0027 ± 0.0002
ΔH_d (kJ/mol)	243 ± 4	257 ± 6	262 ± 2
ΔS_d (J·mol/K)	762 ± 12	808 ± 19	828 ± 6

Table 1: Parameters of the dimer dissociation of inhibitor in xylene at different inhibitor concentrations based on curve fitting.

More information about the interactions are obtained if the net interaction enthalpy per mole of inhibitor molecules are plotted as a function of the mole ratio of inhibitor and *whole* asphaltenes (figure 5). The molar mass of asphaltenes is assumed to be 750 g/mol in agreement with the data by Groenzin and Mullins[33]. Figure 5 shows that all the data obtained at various inhibitor concentrations can be superimposed on a single master curve. The figure also shows that absolute enthalpy values decrease nearly linearly up to inhibitor/asphaltene mole ratio close to 0.06, and then the curve levels off reaching very low values of heat of interaction. This curve could mean that only a small fraction of the asphaltenes, representing only approximately 6 % of the *whole* asphaltenes, would significantly interact with the fatty amine-based inhibitor. The other ca. 94 % of the *whole* asphaltenes would interact much less with the inhibitor as showed by the low absolute values of net interaction heat above an inhibitor/asphaltene mole ratio of approximately 0.07. This distinction between strongly interacting asphaltene fraction and weakly interacting asphaltene fraction is, of course, an oversimplification of the reality since it can be seen that the absolute net heat of interaction decreases when the inhibitor/asphaltene mole ratio increases.

Figure 5 can also be compared with previously reported results concerning the interactions between asphaltenes and long chain carboxylic acids such as tetrameric acids and stearic acids[20]. Indeed, the variations of the net interaction enthalpy per mole of carboxylic acid function as a function of long chain carboxylic acid/asphaltenes mole ratio present

similar variations as for the asphaltenes/inhibitor system. This could mean that in all these systems, a small fraction of asphaltenes interact with the single molecules tested.

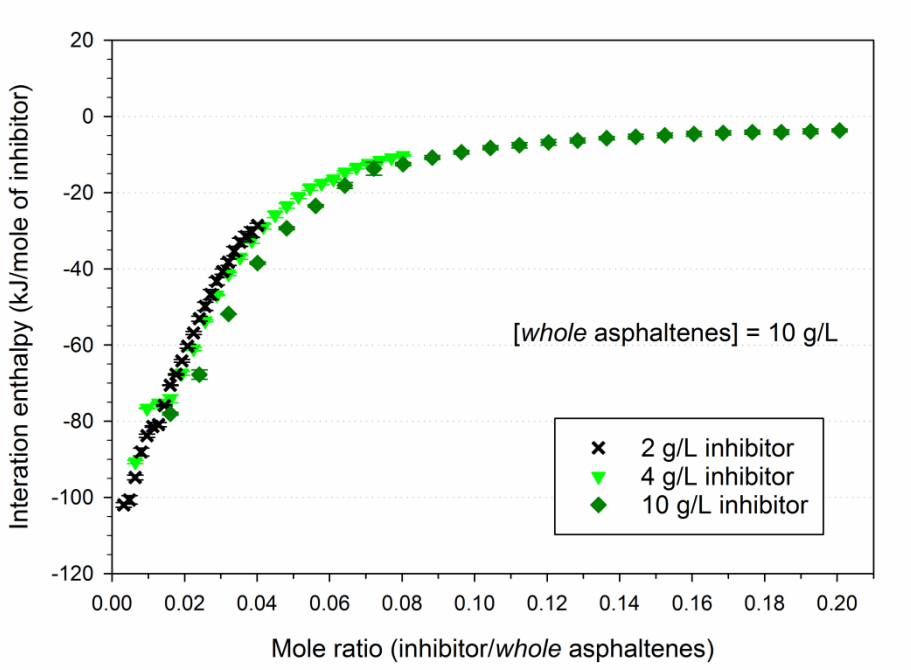

Figure 5: Net interaction enthalpy per mole of inhibitor as a function of mole ratio of inhibitor/*whole* asphaltenes during titration of *whole* asphaltene solution (10 g/L) with inhibitor of different concentrations.

3.2 Interactions between inhibitor and asphaltenes fractions

3.2.1 Interactions studied by ITC measurements

In order to determine which part or functionality of the *whole* asphaltenes interact with the fatty amine-based inhibitor, two asphaltene fractions were tested by ITC. These are *irre-ads* asphaltenes and asphaltenes *3.5V*. These fractions incorporate some of the most extreme asphaltenes i.e. the asphaltenes which are the most strongly adsorbed onto calcium carbonate fraction for *irre-ads* asphaltenes, and the first asphaltenes to precipitate from crude oil when diluted with n-hexane for asphaltenes *3.5V*. The bulk and adsorption properties of these fractions have been previously determined.[21-22]

Figure 6 compares the net interaction enthalpy per mole of inhibitor as a function of mole ratio of inhibitor and *whole* asphaltenes or asphaltene fractions. This figure shows that the magnitude of interactions with inhibitor is different between whole asphaltenes, *irre-ads* asphaltenes and asphaltenes *3.5V*. First among the three asphaltene systems, *irre-ads*

asphaltenes present the highest net interaction enthalpy. The variations of the interaction enthalpy with inhibitor/asphaltene mole ratio for *irre-ads* asphaltenes present a first plateau at low ratio (lower than 0.04), which is absent in the case of *whole* asphaltenes, and then a decrease of absolute net interaction enthalpy which tends to level off. This behavior most likely indicates that *irre-ads* asphaltenes contain a higher content of asphaltene compounds (aggregate or molecule) that interact with inhibitor than *whole* asphaltenes.

The values of the interaction enthalpy for asphaltenes *3.5V* are similar to *whole* asphaltenes at inhibitor/asphaltene mole ratio lower than 0.05-0.06 i.e. for asphaltenes that strongly interact with inhibitor. This could mean that the asphaltene population that strongly interacts with inhibitor is the same in both *whole* asphaltenes and asphaltenes *3.5V*. Consequently, that could imply that the fractionation process of asphaltenes based on precipitation using different ratios of n-hexane and crude oil does not enrich or concentrate the population of asphaltenes that strongly interacts with inhibitor in the asphaltenes *3.5V* fraction. At inhibitor/asphaltene mole ratio higher than 0.05-0.06, the net interaction enthalpy is higher in the case of asphaltenes *3.5V* than for *whole* asphaltenes. We do not have satisfactory explanation for this difference.

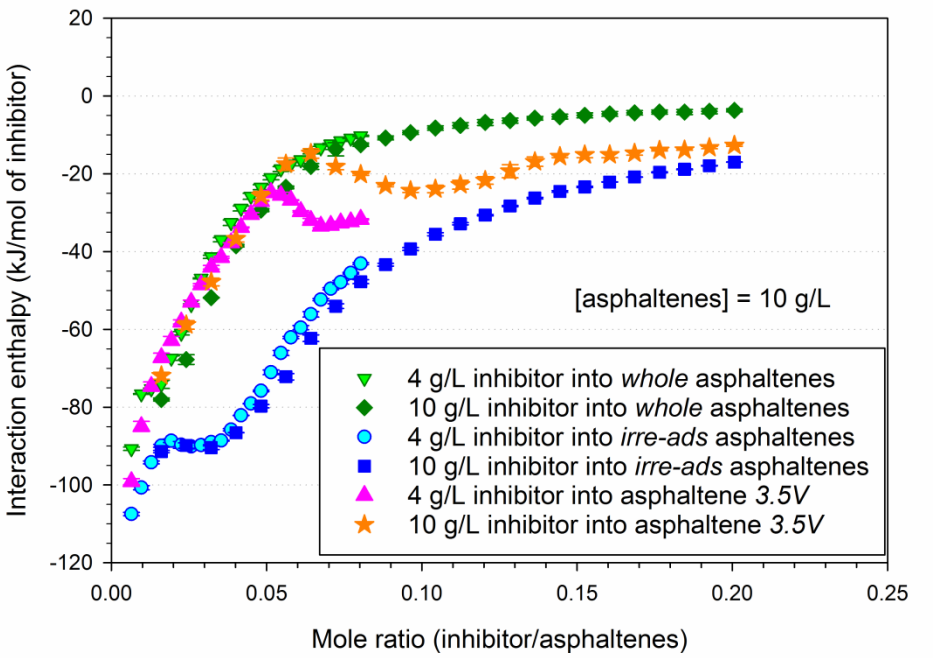

Figure 6: Comparison of net interaction enthalpy per mole of inhibitor as a function of molar ratio of inhibitor/(*whole* asphaltenes or asphaltene fractions) while titrating *whole* asphaltene,

irre-ads asphaltene or asphaltene *3.5V* solution (10 g/L) with different inhibitor concentrations.

3.2.2 Consequences of interactions between asphaltene fractions and inhibitor on precipitation onset

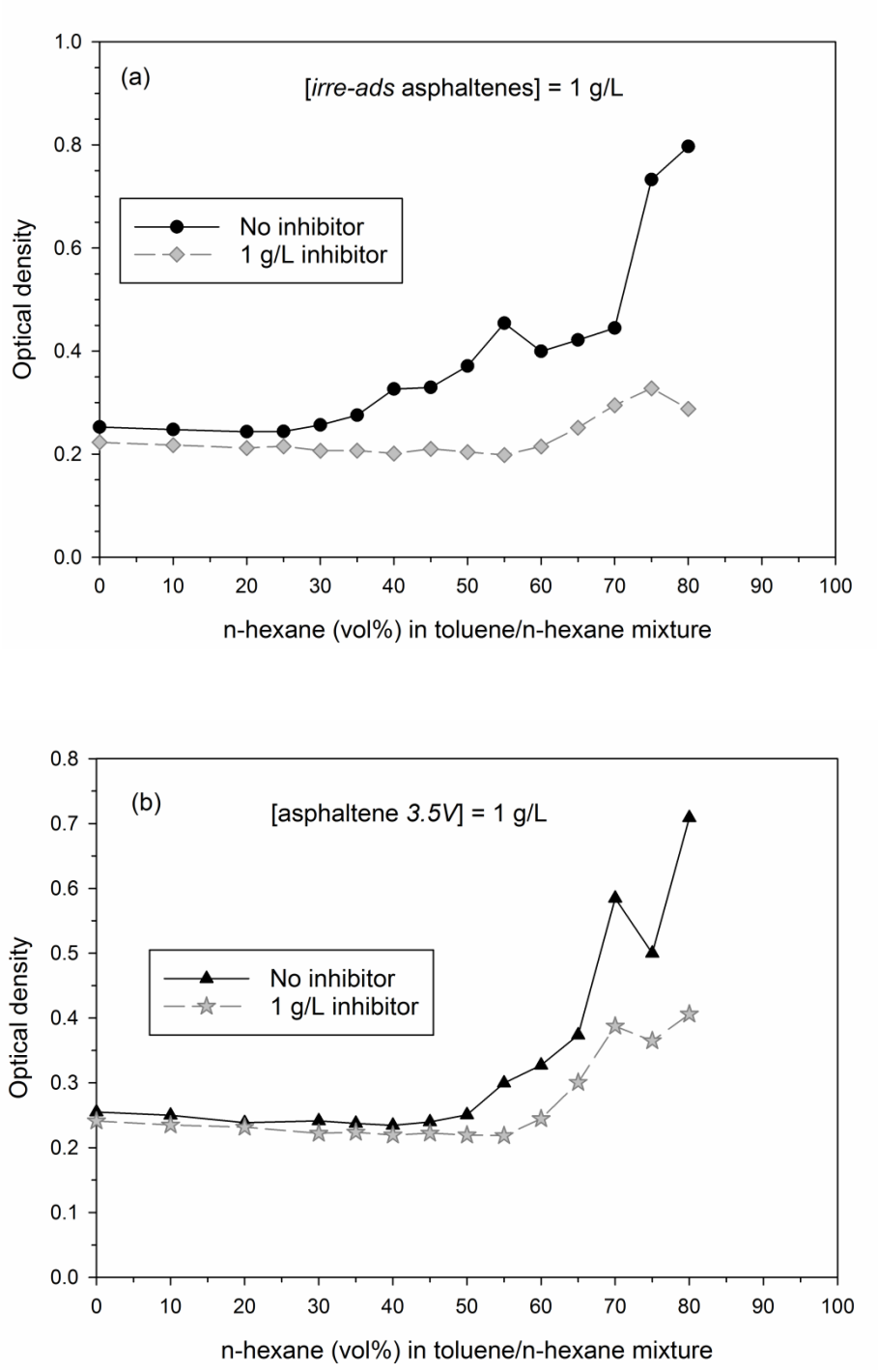

Figure 7: Determination of the precipitation onset of (a) *irre-ads* asphaltene and (b) asphaltene *3.5V* (1 g/L) in mixtures of toluene and n-hexane without and in presence of inhibitor (1 g/L). Measurements performed 1 day after hexane addition at 1600 nm.

Figure 7 shows the determination of the precipitation onset for the fractions (a) *irre-ads* asphaltene and (b) asphaltene *3.5V* both with and without inhibitor. It can be noticed that the inhibitor has only a moderate influence on the precipitation onset of asphaltene *3.5V* fraction with an increase from 40-45 to 55-60 vol% n-hexane in presence of 1 g/L inhibitor. This increase is much higher in the case of the *irre-ads* asphaltene fraction with an increase from 25-30 to 55-60 vol% n-hexane in presence of 1 g/L inhibitor. This indicates that the inhibitor has a much bigger effect on the precipitation onset of *irre-ads* asphaltene fraction

Subramanian et al. have previously compared the composition of *irre-ads* asphaltenes, asphaltenes *3.5V*, and *whole*-asphaltenes in a series of two articles[21-22]. They have noticed by FTIR that *irre-ads* asphaltenes have a higher content of carbonyl groups, such as carboxylic acid and derivative groups, than *whole* asphaltenes. This difference in composition is not observed when asphaltenes *3.5V* and *whole*-asphaltenes are compared. Consequently, it could be hypothesized that the asphaltene population that strongly interacts with inhibitor is composed of asphaltenes containing carbonyl groups and more particularly carboxylic acid groups. This hypothesis will be tested by measuring the interaction enthalpy between esterified asphaltenes and inhibitor in the next section.

3.3 Interactions between inhibitor and *ester*-asphaltenes

3.3.1 Interactions studied by ITC measurements

In order to determine if carboxylic acid-functionalized asphaltenes i.e. acidic asphaltenes are the asphaltene fraction that strongly interacts with inhibitor, *whole*-asphaltenes were esterified by methanol to produce *ester*-asphaltenes. After that, the net interaction enthalpy between *ester*-asphaltenes and the fatty-amine based inhibitor was measured by ITC (figure 8). The shape of the curve presenting the variations of net interaction enthalpy per mole of inhibitor as a function of mole ratio of inhbitor/*ester*-asphaltenes are similar to the *whole* asphaltenes with a sharp decrease of absolute enthalpy then a plateau. However, the absolute enthalpy values obtained in the case of inhibitor/*ester*-asphaltenes interaction are significantly reduced compared with inhibitor/*whole*-asphaltene interactions, and, furthermore the plateau is reached at very low inhibitor/*ester*-asphaltenes ratios (0.015-0.02). This indicates that esterification of *whole*-asphaltenes dramatically decreases the proportion of asphaltenes that interacts strongly with the fatty-amine inhibitor.

The observation therefore confirms that acidic asphaltenes are responsible for most of the interactions with the inhibitor measured by ITC.

The concentration of acidic asphaltenes in an asphaltene sample can, a priori, be determined by acid-base titration. However, the direct determination of the total acid number (TAN) of *whole* asphaltenes via potentiometric titration (TAN standard ASTM D664-95(IP 177/96)[34] and Simon et al.[35]) was not successful owing to the weak solubility of asphaltenes in the toluene/isopropanol/water mixed solvent used for the titration. Consequently, the TAN values for asphaltenes (7.6 mg/g given in Simon et al.[23]) was obtained by the difference between the values determined for crude oil and maltenes. Assuming a molecular weight for asphaltenes of 750 g/mol and 1 carboxylic acid group per asphaltene molecule, it can be calculated that 10 % of asphaltene molecules are acidic. This value is higher than the ratio of asphaltenes interacting with inhibitor determined by ITC in figure 5 but in the same order of magnitude, and this could indicate that not all the acidic asphaltenes interact with inhibitor. This hypothesis however needs further evaluation.

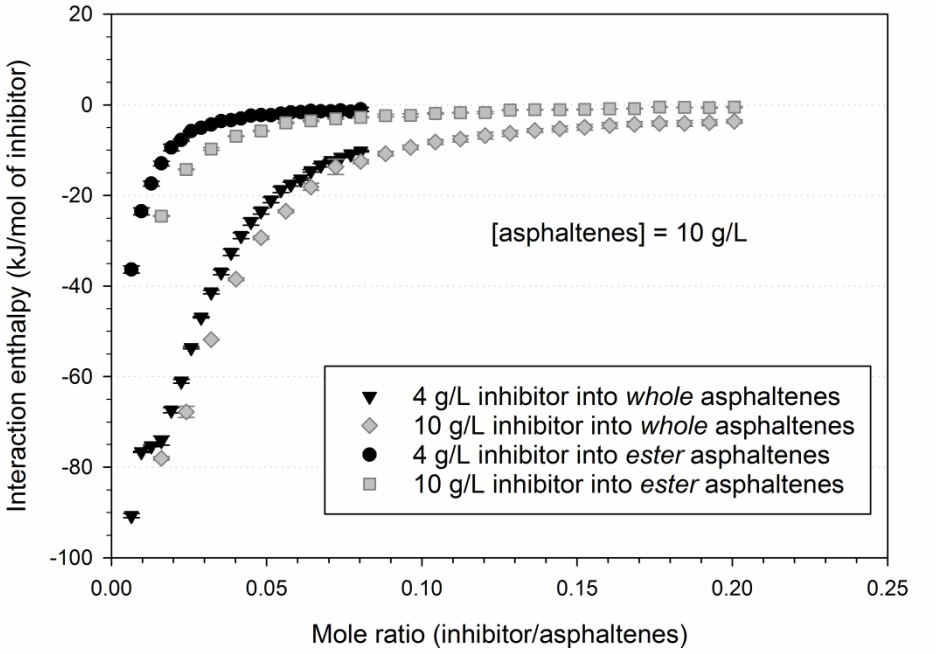

Figure 8: Comparison of net interaction enthalpy per mole of inhibitor as a function of molar ratio of inhibitor/asphaltenes between *whole* asphaltenes *and ester*-asphaltenes. *Whole* or *ester* asphaltene solutions (10 g/L) were titrated by inhibitor solutions of different concentrations (4 or 10 g/L).

In addition, even though it was not the purpose of this article, the *ester*-asphaltene aggregation properties were studied by ITC since the data were required to calculate the net interaction enthalpy presented in figure 8: Experiments were performed by injecting 10 µL aliquots of a 10 g/L *ester*-asphaltene solution in pure xylene. The obtained results are presented in figure 9. The results show that the dilution of *ester*-asphaltenes is an endothermic process which originates from the dissociation of *ester*-asphaltene aggregates. Similar to the inhibitor, the enthalpy data can be satisfactory fitted with a dimer dissociation model. The fitted values of K_d (0.012 ± 0.001 M) and enthalpy of dimer dissociation (4.0 ± 0.1 kJ/mol) are significantly lower than the values for *whole* asphaltenes in xylene (0.019 ± 0.001 M and 6.1 ± 0.1 kJ/mol respectively), but they are not equal to zero. This means that carboxylic acid groups present in asphaltenes are partially responsible, via the formation of hydrogen bonds, for the aggregation of asphaltenes. However, other functionalities are also involved in the formation of the asphaltene nanoaggregates. Similar reduction in heat adsorption in ITC was observed by Merino-Garcia and Andersen[36] for methylated asphaltenes.

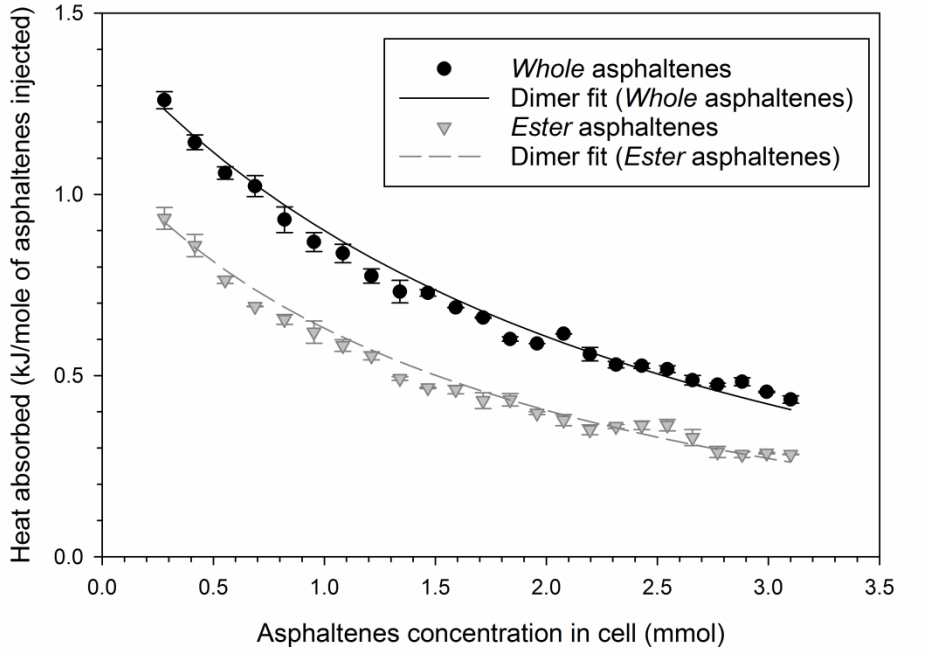

Figure 9: Comparison of the titration of *whole* asphaltenes (10 g/L) *and ester* asphaltenes (10 g/L) in pure xylene. Lines represent the dimer fitting.

3.3.2 Consequences of interactions between *ester*-asphaltenes and inhibitor on precipitation onset

The precipitation onset of *ester*-asphaltenes (2 g/L) in mixtures of toluene and n-hexane has been determined by NIR and shown in figure 10. It increases from 55-60 vol% without inhibitor to 65-70 vol % n-hexane in presence of 2 g/L inhibitor, indicating an increase of ca. 10 vol % n-hexane. The 10 vol% increase in *ester* asphaltene precipitation onset is similar to the increase observed for *whole* asphaltenes (figure 2). As ITC results presented in figure 9 allows us to expect a big difference between *whole* asphaltenes and *ester*-asphaltenes in presence of inhibitor, it was decided to also determine if the inhibitor influences the amount of *whole* asphaltenes and *ester*-asphaltenes precipitated (figure 11). As previously noticed (section 3.1.1), the precipitation onset determined from the percent of precipitated asphaltene values are consistent with NIR data (figure 2, 10 and 11). In addition, figure 11 shows that the variation of amount of precipitated *ester*-asphaltenes as a function of the n-hexane content is similar to *whole* asphaltenes. The influence of inhibitor on the amount of precipitated *ester*-asphaltenes is also similar to *whole* asphaltenes with a shift of values of amount of precipitated asphaltenes by approximately 10 vol% n-hexane. This similarity is even strengthened if the figure 11 is replotted with the n-hexane (vol%) at the precipitation point of asphaltenes (i.e., 60 vol% n-hexane for *whole* asphaltenes and 55 vol% n-hexane for *ester*-asphaltenes) in absence of inhibitor considered as reference point (i.e., zero) as shown in figure 12. This means that fatty-amine based inhibitor has the same flocculation and precipitation effects on acidic and non-acidic asphaltenes. Consequently, there exists interactions between asphaltenes and the tested inhibitor other than acid-base ones that are responsible for the asphaltene precipitation inhibition activity of the inhibitor. These interactions are strangely not detected in the ITC experiments, but the functionalities responsible for the "other" interactions are more concentrated in the of *irre-ads* asphaltene fractions as shown in figure 7. The nature of these interactions is for the moment unknown, but it is thought that it could be related to the presence of other polar functionalities present in asphaltenes (such as phenol, pyridine, pyrrole…). However, more works are required to prove or disprove this hypothesis.

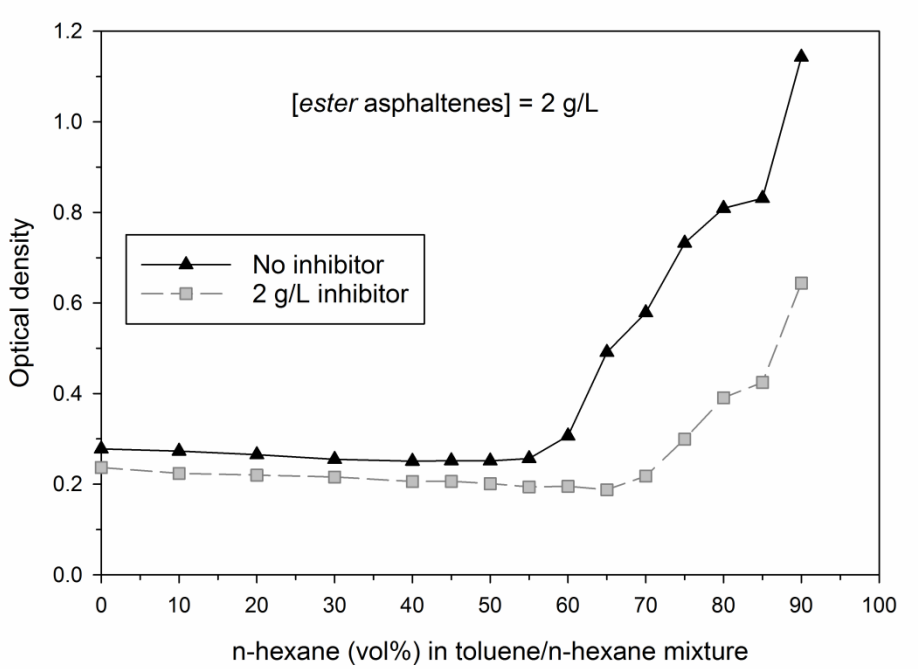

Figure 10: Determination of the precipitation onset of *ester*-asphaltenes (2 g/L) in mixtures of toluene and n-hexane without and in presence of 2 g/L of inhibitor. Measurements performed 1 day after hexane addition at 1600 nm.

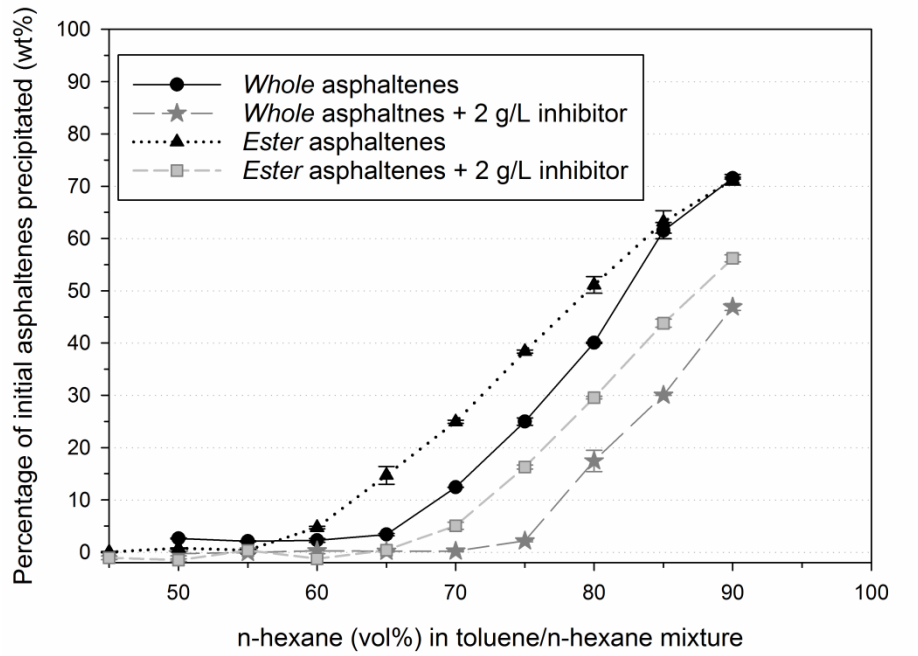

Figure 11: Percentage of *whole*-asphaltenes (2 g/L) and *ester*-asphaltenes (2 g/L) precipitated with and without inhibitor (2 g/L) at various toluene/n-hexane ratios. Initial concentration of asphaltenes was 2 g/L.

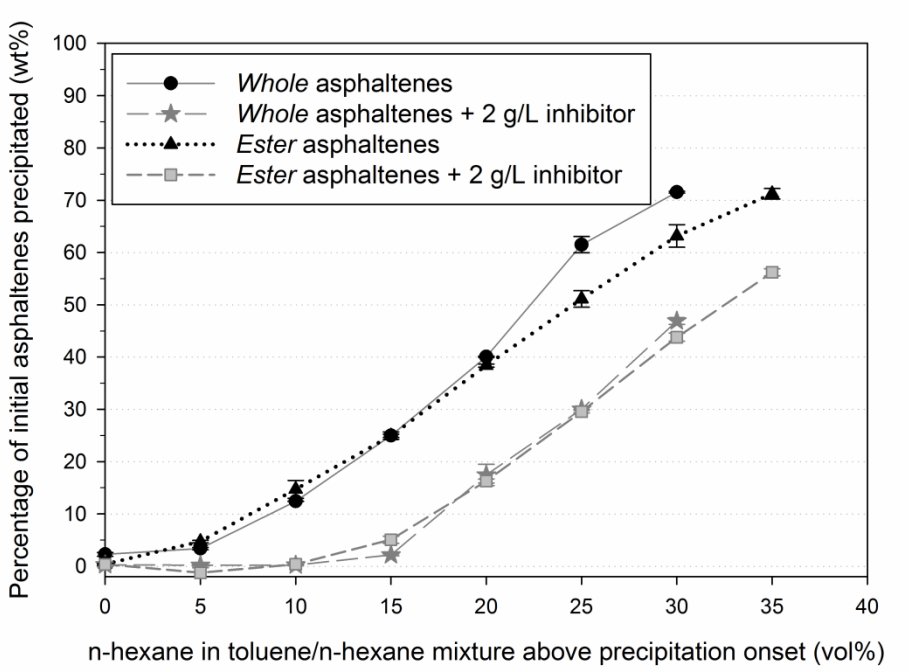

Figure 12: Replotted Figure 11 with the n-hexane (vol%) at the precipitation point of asphaltenes in absence of inhibitor considered as reference point (i.e., zero)

3.4 Conclusion

The goal of this article was to determine the nature of interactions existing between asphaltenes and a commercial fatty amine-based inhibitor. This task was undertaken by measuring "macro" properties such as the asphaltene precipitation onset and the amount of asphaltene precipitated in mixture of solvent/precipitant and quantifying the heat of interactions between asphaltenes and the inhibitor by ITC.

ITC results show that acid-base interaction between inhibitor and asphaltenes does exist. However, they are not the main interaction responsible for the inhibition of asphaltene flocculation/precipitation induced by the inhibitor. Other type(s) of interaction is/are responsible for the inhibition properties of the inhibitor. The nature of other interactions is not known for the moment but it was shown that one of the fraction prepared in this study (*irre-ads* asphaltene fractions) interacts more with asphaltenes, and therefore contains a higher concentration of the functionality(ies) responsible for the "other" type of interaction.

4 Acknowledgments

The authors thank the JIP Asphaltene consortium ''Improved Mechanism of Asphaltene Deposition, Precipitation and Fouling to Minimize Irregularities in Production and Transport (NFR PETROMAKS)'', consisting of Ugelstad Laboratory (NTNU, Norway),

University of Alberta (Canada), University of Pau (France), University of Parana (Brazil) and funded by Norwegian Research Council (grant 234112) and the following industrial sponsors – AkzoNobel, BP, Canada Natural Resources, Nalco Champion, Petrobras, Statoil, and Total E&P Norge AS. The authors thank Hans Oskarsson and Per-Erik Hellberg (AkzoNobel) for providing the inhibitor.

5 References

1. Speight, J. G. Asphaltene Constituents. In *The Chemistry and Technology of Petroleum, Fourth Edition*; CRC Press: Boca Raton, FL, **2006**, pp 315-344.

2. Mullins, O. C. The Asphaltenes. *Annual Review of Analytical Chemistry* **2011,** *4* (1), 393-418.

3. Buckley, J. S.; Hirasaki, G. J.; Liu, Y.; Von Drasek, S.; Wang, J. X.; Gill, B. S. Asphaltene Precipitation and Solvent Properties of Crude Oils. *Petroleum Science and Technology* **1998,** *16* (3-4), 251-285.

4. Yarranton, H. W.; Ortiz, D. P.; Barrera, D. M.; Baydak, E. N.; Barré, L.; Frot, D.; Eyssautier, J.; Zeng, H.; Xu, Z.; Dechaine, G.; Becerra, M.; Shaw, J. M.; McKenna, A. M.; Mapolelo, M. M.; Bohne, C.; Yang, Z.; Oake, J. On the Size Distribution of Self-Associated Asphaltenes. *Energy & Fuels* **2013,** *27* (9), 5083-5106.

5. Laux, H.; Rahimian, I.; Butz, T. Thermodynamics and mechanis of stabilization and precipitation of petroleum colloids. *Fuel Processing Technology* **1997,** *53* (1), 69-79.

6. Rogel, E.; Leon, O.; Espidel, Y.; Gonzalez, Y. Asphaltene Stability in Crude Oils. *SPE Production & Facilities* **2001,** *16* (02), 84-88.

7. Östlund, J.-A.; Nydén, M.; Scott Fogler, H.; Holmberg, K. Functional groups in fractionated asphaltenes and the adsorption of amphiphilic molecules. *Colloids and Surfaces A: Physicochemical and Engineering Aspects* **2004,** *234* (1–3), 95-102.

8. Kelland, M. A. Asphaltene Control. In *Production Chemicals for the Oil and Gas Industry, Second Edition*; CRC Press: Boca Raton, FL, **2014**, pp 111-144.

9. Chang, C.-L.; Fogler, H. S. Stabilization of Asphaltenes in Aliphatic Solvents Using Alkylbenzene-Derived Amphiphiles. 1. Effect of the Chemical Structure of Amphiphiles on Asphaltene Stabilization. *Langmuir* **1994,** *10* (6), 1749-1757.

10. Chang, C.-L.; Fogler, H. S. Stabilization of Asphaltenes in Aliphatic Solvents Using Alkylbenzene-Derived Amphiphiles. 2. Study of the Asphaltene-Amphiphile Interactions and Structures Using Fourier Transform Infrared Spectroscopy and Small-Angle X-ray Scattering Techniques. *Langmuir* **1994,** *10* (6), 1758-1766.

11. Goual, L.; Sedghi, M.; Wang, X.; Zhu, Z. Asphaltene Aggregation and Impact of Alkylphenols. *Langmuir* **2014,** *30* (19), 5394-5403.

12. Chang, C.-L.; Fogler, H. S. Asphaltene Stabilization in Alkyl Solvents Using Oil-Soluble Amphiphiles (SPE-25185-MS). In *SPE International Symposium on Oilfield Chemistry, 2-5 March*; Society of Petroleum Engineers: New Orleans, Louisiana, **1993**.

13. Clarke, P. F.; Pruden, B. B. Asphaltene Precipitation from Cold Lake and Athabasca Bitumens. *Petroleum Science and Technology* **1998,** *16* (3-4), 287-305.

14. León, O.; Rogel, E.; Urbina, A.; Andújar, A.; Lucas, A. Study of the Adsorption of Alkyl Benzene-Derived Amphiphiles on Asphaltene Particles. *Langmuir* **1999,** *15* (22), 7653-7657.

15. Wiehe, I. A.; Jermansen, T. G. Design of Synthetic Dispersants for Asphaltenes. *Petroleum Science and Technology* **2003,** *21* (3-4), 527-536.

16. Wang, J.; Li, C.; Zhang, L.; Que, G.; Li, Z. The Properties of Asphaltenes and Their Interaction with Amphiphiles. *Energy & Fuels* **2009,** *23* (7), 3625-3631.

17. Goual, L.; Firoozabadi, A. Effect of resins and DBSA on asphaltene precipitation from petroleum fluids. *AIChE Journal* **2004,** *50* (2), 470-479.

18. Barcenas, M.; Orea, P.; Buenrostro-González, E.; Zamudio-Rivera, L. S.; Duda, Y. Study of Medium Effect on Asphaltene Agglomeration Inhibitor Efficiency. *Energy & Fuels* **2008,** *22* (3), 1917-1922.

19. Merino-Garcia, D.; Andersen, S. I. Interaction of Asphaltenes with Nonylphenol by Microcalorimetry. *Langmuir* **2004,** *20* (4), 1473-1480.

20. Wei, D.; Orlandi, E.; Simon, S.; Sjöblom, J.; Suurkuusk, M. Interactions between asphaltenes and alkylbenzene-derived inhibitors investigated by isothermal titration calorimetry. *Journal of Thermal Analysis and Calorimetry* **2015,** *120* (3), 1835-1846.

21. Subramanian, S.; Simon, S.; Gao, B.; Sjöblom, J. Asphaltene fractionation based on adsorption onto calcium carbonate: Part 1. Characterization of sub-fractions and QCM-D measurements. *Colloids and Surfaces A: Physicochemical and Engineering Aspects* **2016,** *495*, 136-148.

22. Subramanian, S.; Sørland, G. H.; Simon, S.; Xu, Z.; Sjöblom, J. Asphaltene fractionation based on adsorption onto calcium carbonate: Part 2. Self-association and aggregation properties. *Colloids and Surfaces A: Physicochemical and Engineering Aspects* **2017,** *514*, 79-90.

23. Simon, S.; Sjöblom, J.; Wei, D. Interfacial and Emulsion Stabilizing Properties of Indigenous Acidic and Esterified Asphaltenes. *Journal of Dispersion Science and Technology* **2016,** *37* (12), 1751-1759.

24. Pradilla, D.; Subramanian, S.; Simon, S.; Sjöblom, J.; Beurroies, I.; Denoyel, R. Microcalorimetry Study of the Adsorption of Asphaltenes and Asphaltene Model Compounds at the Liquid–Solid Surface. *Langmuir* **2016,** *32* (29), 7294-7305.

25. Nasir, S.; Mansir, N.; Augie, N. M. Geochemical Study of Crude Oil Samples to Evaluate Extent and Effect of Secondary Alteration Process (ie Biodegradation). *International Journal of Scientific and Research Publications* **2014**, 169.

26. Maqbool, T.; Srikiratiwong, P.; Fogler, H. S. Effect of temperature on the precipitation kinetics of asphaltenes. *Energy & Fuels* **2011,** *25* (2), 694-700.

27. Yudin, I.; Nikolaenko, G.; Gorodetskii, E.; Kosov, V.; Melikyan, V.; Markhashov, E.; Frot, D.; Briolant, Y. Mechanisms of asphaltene aggregation in toluene–heptane mixtures. *Journal of Petroleum Science and Engineering* **1998,** *20* (3), 297-301.

28. Anisimov, M.; Yudin, I.; Nikitin, V.; Nikolaenko, G.; Chernoutsan, A.; Toulhoat, H.; Frot, D.; Briolant, Y. Asphaltene aggregation in hydrocarbon solutions studied by photon correlation spectroscopy. *The Journal of Physical Chemistry* **1995,** *99* (23), 9576-9580.

29. Spiecker, P. M.; Gawrys, K. L.; Trail, C. B.; Kilpatrick, P. K. Effects of petroleum resins on asphaltene aggregation and water-in-oil emulsion formation. *Colloids and Surfaces A: Physicochemical and Engineering Aspects* **2003,** *220* (1–3), 9-27.

30. Ghloum, E. F.; Al-Qahtani, M.; Al-Rashid, A. Effect of inhibitors on asphaltene precipitation for Marrat Kuwaiti reservoirs. *Journal of Petroleum Science and Engineering* **2010,** *70* (1–2), 99-106.

31. Al-Sahhaf, T. A.; Fahim, M. A.; Elkilani, A. S. Retardation of asphaltene precipitation by addition of toluene, resins, deasphalted oil and surfactants. *Fluid Phase Equilibria* **2002,** *194–197*, 1045-1057.

32. Allenson, S. J.; Walsh, M. A. In *A novel way to treat asphaltene deposition problems found in oil production (SPE-37286-MS)*, International Symposium on Oilfield Chemistry, 18-21 February, , Houston, Texas, **1997**; Society of Petroleum Engineers, pp 699 - 702.

33. Groenzin, H.; Mullins, O. C. Molecular Size and Structure of Asphaltenes from Various Sources. *Energy & Fuels* **2000,** *14* (3), 677-684.

34. ASTM D664-95 (IP 177/96): Standard Test Method for Acid Number of Petroleum Products by Potentiometric Titration.; American Society for Testing Materials (ASTM) Philadelphia, **2005**.

35. Simon, S.; Nenningsland, A. L.; Herschbach, E.; Sjöblom, J. Extraction of Basic Components from Petroleum Crude Oil. *Energy & Fuels* **2010,** *24* (2), 1043-1050.

36. Merino-Garcia, D.; Andersen, S. I. Application of isothermal titration calorimetry in the investigation of asphaltene association. In *Asphaltenes, Heavy Oils, and Petroleomics*; Springer, **2007**, pp 329-352.